NANOMEDICINE

A Dense Poly(Ethylene Glycol) Coating Improves Penetration of Large Polymeric Nanoparticles Within Brain Tissue

Elizabeth A. Nance,[1,2]* Graeme F. Woodworth,[1,3]* Kurt A. Sailor,[4] Ting-Yu Shih,[2] Qingguo Xu,[1,5] Ganesh Swaminathan,[2] Dennis Xiang,[2] Charles Eberhart,[1,5,6] Justin Hanes[1,2,3,5]†

Prevailing opinion suggests that only substances up to 64 nm in diameter can move at appreciable rates through the brain extracellular space (ECS). This size range is large enough to allow diffusion of signaling molecules, nutrients, and metabolic waste products, but too small to allow efficient penetration of most particulate drug delivery systems and viruses carrying therapeutic genes, thereby limiting effectiveness of many potential therapies. We analyzed the movements of nanoparticles of various diameters and surface coatings within fresh human and rat brain tissue ex vivo and mouse brain in vivo. Nanoparticles as large as 114 nm in diameter diffused within the human and rat brain, but only if they were densely coated with poly(ethylene glycol) (PEG). Using these minimally adhesive PEG-coated particles, we estimated that human brain tissue ECS has some pores larger than 200 nm and that more than one-quarter of all pores are ≥100 nm. These findings were confirmed in vivo in mice, where 40- and 100-nm, but not 200-nm, nanoparticles spread rapidly within brain tissue, only if densely coated with PEG. Similar results were observed in rat brain tissue with paclitaxel-loaded biodegradable nanoparticles of similar size (85 nm) and surface properties. The ability to achieve brain penetration with larger nanoparticles is expected to allow more uniform, longer-lasting, and effective delivery of drugs within the brain, and may find use in the treatment of brain tumors, stroke, neuroinflammation, and other brain diseases where the blood-brain barrier is compromised or where local delivery strategies are feasible.

INTRODUCTION

The blood-brain barrier (BBB) has long been considered an impediment for effective treatment and imaging of a broad range of central nervous system (CNS) diseases (*1*). As a result, localized strategies for delivering substances within the brain have become important (*2*). For example, Gliadel, a biodegradable polymer wafer loaded with carmustine that is implanted in the brain after tumor resection, was approved by the U.S. Food and Drug Administration in 1996 for treatment of patients with recurrent glioblastomas (GBMs). This therapy improves survival of patients with GBM and high-grade glioma, and demonstrates the importance of locally administered, controlled-release polymer systems in treating brain tumors.

The BBB is also known to be disrupted by the presence of brain tumors and in other clinical situations, including during neuroinflammation, abnormal development, infection, and cerebrovascular disease (stroke, hypertension, and ischemia) (*1*, *3*). BBB breakdown in these cases allows drugs and drug-loaded nanoparticles (NPs) up to a few hundred nanometers in diameter to bypass the endothelium that comprises the BBB and enter the brain, for example, by the enhanced permeation and retention (EPR) effect (*4*) in tumors and at sites of inflammation. Systemic drug delivery to the CNS by NPs in these cases has been shown to have positive therapeutic effects in various animal disease models, including brain tumors (*5*), neuroinflammation (*6*), and ischemia (*7*). In addition, it has been shown that NPs coated with poly(ethylene glycol) (PEG) accumulate more efficiently in the brain with a compromised BBB compared to similar uncoated NPs (*8*, *9*), at least partly as a result of the greatly improved blood circulation time and the "stealth" nature of PEG-coated particles (*10*).

Methods that improve drug penetration within the brain parenchyma (*11*) have also been shown to enhance therapeutic efficacy in animal models. For example, localized convection-enhanced delivery (CED) has been used to widely distribute drugs (*12*), macromolecules (*13*), and nanocarriers (*14*) in the brain, leading to enhanced efficacy compared to systemic therapy. In addition, Pluen *et al.* have shown that the EPR effect is heterogeneous in tumors and that increased interstitial pressure in tumors can limit drug penetration (*15*), thereby motivating the need for NPs that can penetrate parenchyma once within the brain. However, it has been suggested that NPs must be very small (<64 nm) to penetrate within the brain parenchyma through the extracellular space (ECS) (*16*). Openings below this size are large enough to allow diffusion of proteins and small molecules, while being small enough to limit the movement of many nanoparticulate drug delivery or imaging systems. Thus, despite the need to deliver drugs directly to brain tissue, the human brain ECS is thought to pose a formidable barrier to NP penetration.

We therefore sought to determine whether dense coatings with low–molecular weight PEG might allow larger NPs (up to 200 nm) to penetrate the brain parenchyma. The ability to achieve brain penetration with larger NPs will enable higher drug-loading efficiency and payload, greater dispersion of drugs, and longer drug release—factors that enhance translational potential of any nanotherapeutic approach because of the known correlation with efficacy (*17*). We used rodent

[1]Center for Nanomedicine at the Wilmer Eye Institute, Johns Hopkins University School of Medicine, Baltimore, MD 21231, USA. [2]Department of Chemical and Biomolecular Engineering, Johns Hopkins University, Baltimore, MD 21218, USA. [3]Department of Neurosurgery, Johns Hopkins University School of Medicine, Baltimore, MD 21205, USA. [4]Department of Neuroscience, Institute for Cellular Engineering, Johns Hopkins University School of Medicine, Baltimore, MD 21205, USA. [5]Department of Ophthalmology, The Wilmer Eye Institute, Johns Hopkins University School of Medicine, Baltimore, MD 21231, USA. [6]Department of Pathology, The Wilmer Eye Institute, Johns Hopkins University School of Medicine, Baltimore, MD 21231, USA.
*These authors contributed equally to this work.
†To whom correspondence should be addressed. E-mail: hanes@jhu.edu

brain tissue in vivo and ex vivo, and fresh human tissue ex vivo, to study brain ECS pore size and NP diffusion within the brain. Real-time multiple particle tracking (MPT) indicated that NPs at least 114 nm in diameter were capable of penetrating human and rat brain tissue. In support of these findings, the movements of the same NPs in the living mouse brain were directly visualized and compared with in vivo particle tracking through a cranial window. A paclitaxel-loaded NP system with similar size and surface characteristics as the conventional PEG-coated particles showed that therapeutic delivery for CNS disorders is possible.

RESULTS

Particle tracking in human brain tissue ex vivo

Having previously shown that transport of unexpectedly large NPs through mucus gels depends on their surface coatings (*18*, *19*), we hypothesized here that similar modifications of particle physicochemical properties could provide a more accurate estimate of the pore size range within the human brain ECS. Fluorescent polystyrene (PS) particles with dense PEG or carboxyl (COOH) coatings (Table 1) were added to freshly dissected human brain cortex tissue, and the particle Brownian motions were quantified with ex vivo high-resolution MPT (Supplementary Methods). The PEG-coated particles used were 10 to 20 nm larger than the COOH-coated particles and had a near-neutral net surface charge (Table 1). PEG-coated PS particles have surfaces dominated by PEG, which prevents aggregation in artificial cerebrospinal fluid (ACSF), as indicated by the low polydispersity index (PDI) values provided in Table 1. The 40- and 100-nm PEG-coated particles rapidly penetrated human brain tissue, as exhibited by ensemble geometric mean square displacements (MSDs) that were 2300- and 1500-fold higher than similarly sized COOH-coated particles (Fig. 1A and Table 1). PEG-coated 40- and 100-nm particles diffused only 37 and 36 times slower, respectively, in the human brain tissue ex vivo than in ACSF, whereas standard COOH-coated PS particles of similar sizes moved 54,000 to 86,000 times slower in brain than in ACSF (Table 1). Therefore, dense PEG coatings allowed 40- and 100-nm particles to experience the brain ECS as a permeable viscoelastic liquid rather than an impermeable viscoelastic solid, as seen previously with PEGylated NPs with diameters smaller than the average mesh size in human mucus samples (*18*). The similar, rapid transport rates of 40- and 100-nm PEG-coated particles in the human brain tissue are expected only if the ECS pore size cutoff is greater than 100 nm.

In contrast, 200-nm PEG-coated particles diffused 1600 times slower in the human brain tissue ex vivo than in ACSF, or about 45-fold slower than the 100-nm PEG-coated particles in the brain (Fig. 1A). The expected difference for diffusion rates of 100- and 200-nm particles—defined by a ratio of the theoretical diffusion coefficient D_2/D_1 (where D is defined by the Stokes-Einstein equation)—would be only twofold for nonadhesive NPs, unless there was an ECS pore size cutoff between 100 and 200 nm. The density and viscosity of ACSF are the same as water at physiological pH; therefore, ACSF and water are assumed to be equal for this study. Representative particle trajectories for both PEG- and COOH-coated particles at all sizes studied in human brain tissue are provided in Fig. 1B. COOH-coated particles exhibited highly constrained motion regardless of size, presumably owing to adhesive interactions, whereas the same particles densely coated with PEG exhibited diffusive motion for 40- and 100-nm particles, but hindered motion for 200 nm. For all NP sizes studied, 100% of COOH-coated particles were immobilized (MSDs below the resolution of the microscope) or strongly hindered (MSDs smaller than the particle diameter) within the ECS. These observations suggest that, regardless of PS particle size, electrostatic (negatively charged carboxylate surface) and/or hydrophobic (exposed PS surfaces) interactions limit uncoated NP diffusion within the brain.

To estimate the effective pore size range in the human brain ECS, we fit the Amsden obstruction scaling model (*20*) for entangled and cross-linked gels to the MSD data in Fig. 1A, as shown previously for estimating the pore size in human mucus (*18*, *21*). Human brain tissue ECS was found to have pores as large as 225 nm, with about 28% of the pores larger than 100 nm (Fig. 1C). The smallest pores experienced by the probe particles were less than 40 nm, which is similar to previous reports based on Fick's law–derived diffusion analysis of NPs with lower-density PEG coatings (*16*, *22*, *23*).

Table 1. Physicochemical properties and diffusivity of PS NPs in normal human cortical tissue and in ACSF. Effective diffusivity of NPs in normal brain tissue (D_b) was calculated at a time scale of 1 s. NP diffusivity in ACSF (D_{ACSF}) was calculated with Stokes-Einstein equation and mean particle diameter. Size was provided by the manufacturer, and actual diameter in ACSF at pH 7.0 was measured with dynamic light scattering. ζ potential and PDI were measured in ACSF at pH 7.0. Size, ζ potential, and PDI were all measured after 24-hour incubation in ACSF.

Size (nm)	Surface modification of PS NPs	Mean diameter ± SEM (nm)	Mean ζ potential ± SEM (mV)	PDI	D_{ACSF}/D_b
40	PEG	69 ± 2	−2.8 ± 0.4	0.05	37*
40	COOH	57 ± 2	−39 ± 2.5	0.04	85,000
100	PEG	106 ± 4	−4.4 ± 0.2	0.03	36*
100	COOH	94 ± 3	−31 ± 4.5	0.03	54,000
200	PEG	198 ± 6	−7.8 ± 0.6	0.03	1,600*
200	COOH	185 ± 1	−52 ± 2.6	0.01	86,000

*$P < 0.05$ compared to COOH-PS [analysis of variance (ANOVA)].

Ex vivo tissue integrity during particle tracking

The ex vivo brain slice model has been used extensively to study the diffusion of various substances (*24*), neural electrophysiology (*25*), and cell migration (*26*, *27*). Histological analysis has consistently confirmed intact cytoarchitecture and functioning tissue physiology (*28*, *29*). Representative hematoxylin and eosin (H&E)–stained sections ($n = 4$ sections for each of five patients at both $t = 0$ and 3 hours) of the initial and post-acquisition human brain tissue were examined by a pathologist (C.E.). In particular, the presence of cellular swelling, pyknotic nuclei, and ischemia was examined. No differences were observed in the brain tissue between immediate tissue removal (30 min) and 3 hours after tissue removal (Fig. 1D), suggesting that minimal damage was introduced by tissue removal, collection, and processing. All particle-tracking experiments were conducted within this time frame.

Particle tracking in live mouse brain

The ex vivo model is limited in that it is not subject to the dynamic environment of the living brain, including the bulk flow of cerebro-

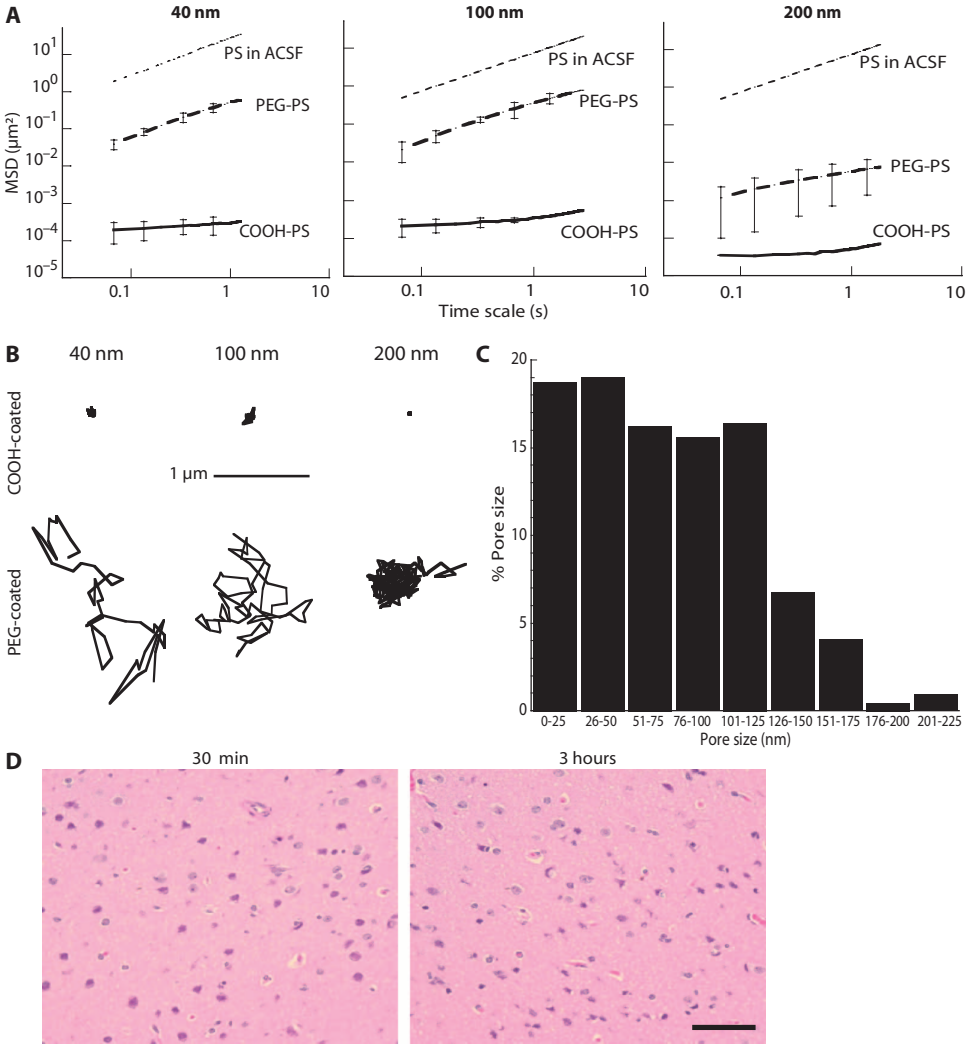

Fig. 1. NP penetration of human brain tissue ex vivo. (**A**) Ensemble-averaged geometric MSDs as a function of time scale for 40-, 100-, and 200-nm PEG- and COOH-coated PS NPs. Data represent the ensemble average of at least four independent experiments, with $n \geq 100$ particles for each experiment. For each experiment, the transport rates of all three particle sizes, with and without PEG coatings, were measured in the same brain tissue. Gray dotted lines indicate theoretical diffusivity values based on Stokes-Einstein equation for the same size particles in ACSF. (**B**) Representative particle trajectories for COOH- and PEG-coated NPs of various sizes in human brain tissue. Trajectories shown are of particles that had an MSD equal to the ensemble average at a time scale of 1 s. (**C**) Percent of pores that fall in a dedicated size range in the ECS of fresh human brain tissue. Pore size distribution approximation was based on diffusion rates of PEG-coated 100-nm NPs combined with an obstruction scaling model (*14*). Data represent the ensemble average of four independent experiments with $n >$ 100 particles tracked for each experiment. (**D**) H&E-stained human cortical brain slices 30 min after removal and after MPT for 3 hours ex vivo in culture at 37°C. Scale bar, 40 μm.

spinal fluid and ECS volume fraction changes that can occur. Therefore, using live-animal imaging, we directly observed NP penetration in vivo in mouse brains to confirm findings obtained using ex vivo tissue slices. Red fluorescent, COOH-coated NPs and green fluorescent, PEG-coated NPs with similar diameters were co-injected into the mouse cerebral cortex at a depth of 100 to 200 μm below the pial surface. Real-time video microscopy showed that COOH-coated particles of all sizes were uniformly stuck in the tissue, whereas 40- and 100-nm particles with dense PEG coatings penetrated up to 200 μm into the tissue within the 60-min imaging interval (Fig. 2A). PEG-coated 200-nm particles did not penetrate the brain tissue, presumably because of steric hindrance.

To further confirm these differences between size and particle coating, we performed co-injections 100 to 200 μm below the pial surface of PEG-coated red and green fluorescent NPs of different sizes. Similar to results observed in the human brain tissue ex vivo, the 40- and 100-nm PEG-coated particles penetrated farther into the mouse brain in vivo than the 200-nm PEG-coated particles (Fig. 2B), confirming relatively few ECS pores greater than 200 nm. Representative single-particle trajectories from separate regions within the brain showed much farther movement for the 100-nm PEG-coated particles compared to either the PEG-coated 200-nm particles or the COOH-coated 100- and 200-nm particles (Fig. 2C). We were unable to consistently resolve the individual movements of 40-nm PEG-coated particles in vivo owing to their exceptionally fast movement in and out of the focal plane.

Drug-loaded biodegradable NPs in rat brain tissue ex vivo

Biodegradable NP systems composed of block copolymers of poly(lactic-*co*-glycolic acid) (PLGA) and PEG and loaded with paclitaxel could rapidly diffuse in normal rat brain tissue ex vivo, whereas PLGA NPs without PEG coatings could not (movies S1 and S2). Representative particle trajectories of paclitaxel-loaded PEG-PLGA NPs (mean ± SEM: 85 ± 3 nm; −2.7 ± 0.5 mV; 2.5 weight percent paclitaxel), PEG-PLGA NPs that did not contain drug (mean ± SEM: 78 ± 3 nm; −3.5 ± 1 mV), and uncoated PLGA particles (mean ± SEM: 81 ± 3 nm; −30.1 ± 1 mV) are provided in Fig. 3A.

By examining the distribution of individual particle diffusivities, we established that biodegradable PEG-PLGA NP systems exhibit a more substantial rapidly diffusing fraction (24%) compared to PLGA NP systems (Fig. 3B). The biodegradable systems tested had similar size characteristics compared to the 100-nm PS particles used in our studies here in human brain tissue ex vivo and in living mouse brains.

High PEG surface density required for NP diffusion in brain ECS

We found that a dense PEG coating on PS NPs, quantum dots (QDs), and PLGA NPs, which results in a near-neutral NP surface charge,

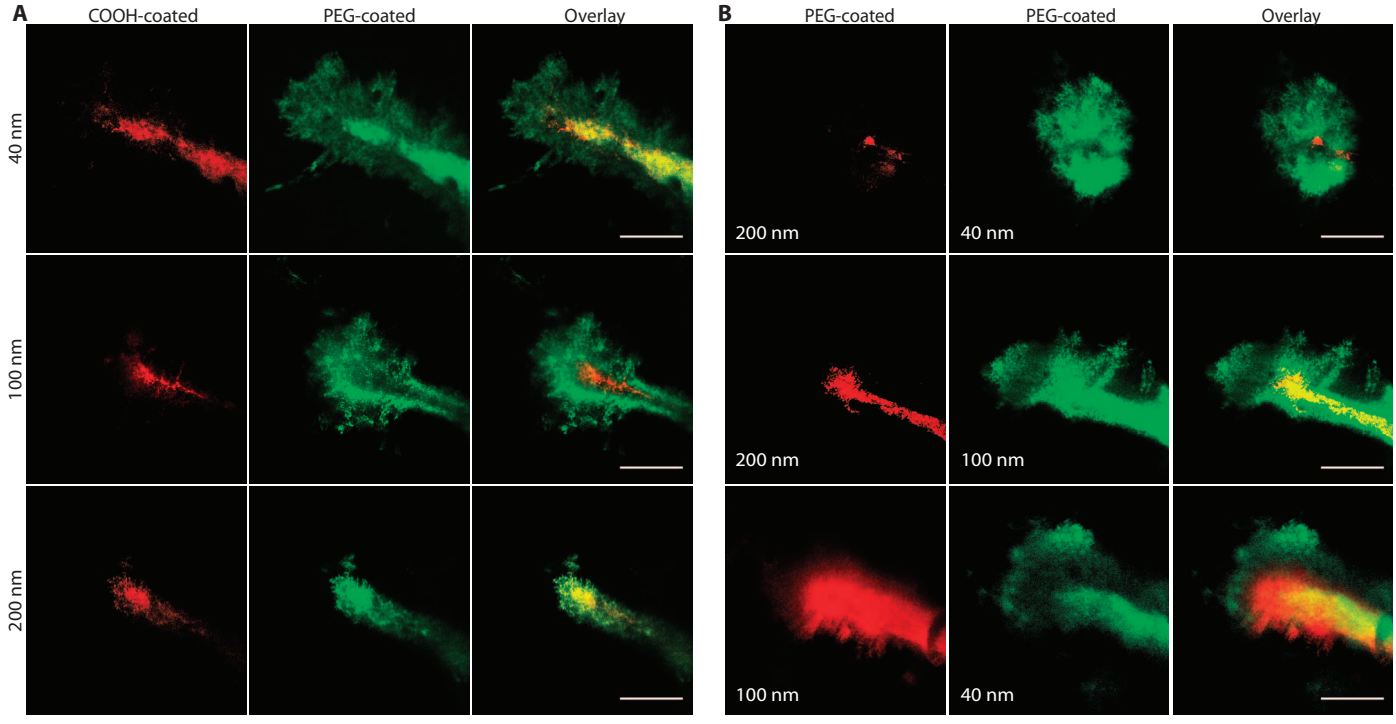

Fig. 2. NP penetration of brain tissue in vivo in living mice. Actual sizes of each particle type are listed in Table 1. (**A**) Direct comparison of the distribution of fluorescent NPs of similar sizes with different surface coatings after intracranial co-injection into mice. Images were acquired 60 min after injection. Scale bars, 50 μm. (**B**) Direct comparison of the distribution of PEG-coated NPs of various sizes after intracranial co-injection into mice. Images were acquired 60 min after injection. Scale bars, 50 μm. (**C**) Representative particle trajectories for COOH- and PEG-coated NPs in live mouse brain. Trajectories shown are of particles that had an MSD equal to the ensemble average at a time scale of 1 s, as determined by at least three independent experiments, with $n \geq 100$ particles tracked for each experiment.

correlated with a greater percent diffusive fraction in rat brain tissue ex vivo (Fig. 4 and Table 2). NP formulations with ζ potentials less negative than −4 mV were consistently capable of diffusing in the rat brain (five of five NP formulations). Conversely, only one of two NP formulations with ζ potentials between −4 and −6 mV had NPs that diffused, and zero of six NP formulations with ζ potentials more negative than −6 mV were capable of diffusion (Fig. 4). Using a nuclear magnetic resonance (NMR)–based method to quantify the PEG coating density required for NPs to diffuse in the brain, we estimate that 100-nm PS NPs must have roughly nine PEG molecules (molecular size, 5 kD) per 100 nm^2 of particle surface to diffuse in the rat brain tissue slice model. NPs that diffused within the brain had PEG layers in the brush regime, with Γ/SA ≥2, where Γ is the total surface area (SA) coverage that would be provided by the PEG molecules assuming that PEG conformation on the particle surface was unconstrained (Supplementary Methods). NP formulations with Γ/SA ≤1.7 did not diffuse in the rat brain slice model.

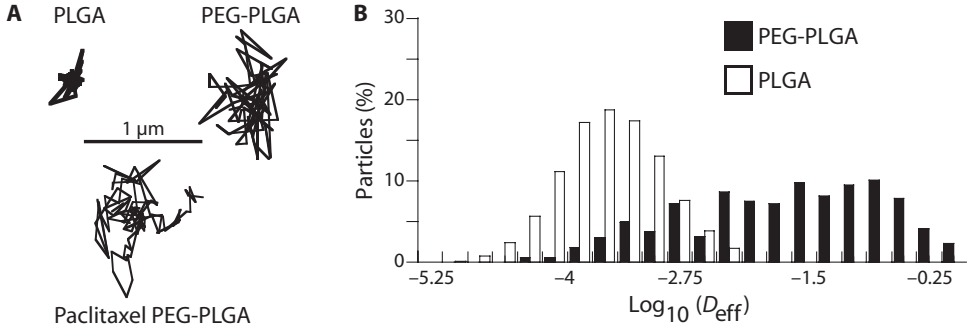

Fig. 3. Transport of paclitaxel-loaded PEG-PLGA NPs through rat brain tissue ex vivo. (**A**) Sample trajectories of PLGA, PEG-PLGA, and paclitaxel-loaded PEG-PLGA NPs in brain tissue. Trajectories reflect particles with effective diffusivities within 1 SEM of the ensemble average. (**B**) Distributions of the logarithms of individual particle effective diffusivities (D_{eff}) for PLGA and PEG-PLGA NPs at a time scale of 1 s. Data represent means of at least three experiments, with $n \geq 100$ particles per experiment.

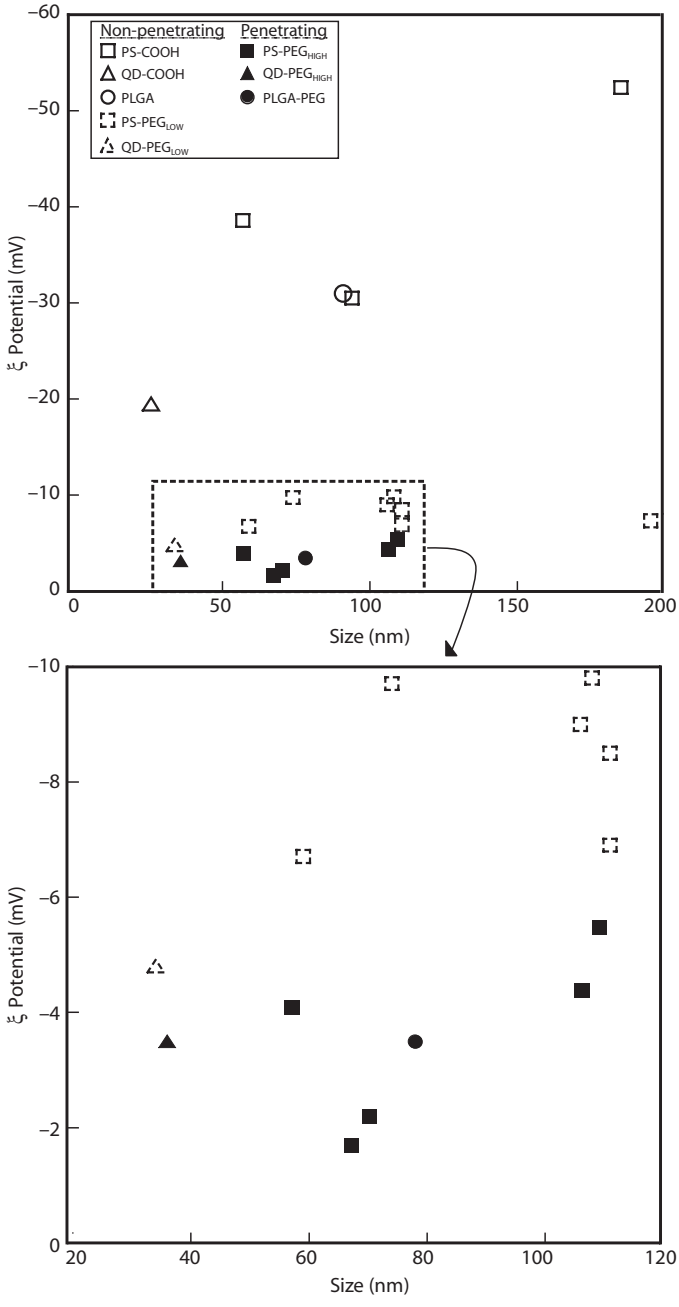

Fig. 4. Phase diagram correlating ζ potential and size to transport behavior. Data were obtained from rodent brain tissue ex vivo for various uncoated and PEG-coated NPs (n = 3). Black-filled symbols indicate diffusive brain-penetrating particles, and open symbols indicate particles that are immobilized. The lower box is an expanded view of the indicated region in dotted box. Each data point represents one NP formulation.

DISCUSSION

Here, MPT was used to analyze the diffusion rates of densely PEG-coated versus standard COOH-coated NPs of various sizes in human and rat brain tissue ex vivo, as well as in the living mouse brain in vivo. The results from three model systems aligned closely, producing surprising results: (i) the human, rat, and mouse brain ECS have 28% of pores ≥100 nm; (ii) particles larger than the previously reported ECS mesh size range (upper limit of 64 nm) (*16*) rapidly penetrate within the brain, but only if densely coated with PEG (Γ/SA ≥ 2), which minimizes adhesive interactions; and (iii) all uncoated NPs—even the 40-nm particles—were essentially immobile in human, rat, and mouse brains. Large brain-penetrating NPs that contain bioactive drugs and are composed of biocompatible molecules, such as PLGA and PEG, with a long history of safe use in humans, should facilitate translation and testing of therapeutic strategies in human clinical trials.

These findings were guided by our previous work defining the particle size and surface chemistry required for NP penetration through another biologic interface. Specifically, by using minimally adhesive NPs with dense PEG coatings, we showed previously that human mucus barriers have pores much larger than expected (*18*, *19*, *21*). Accurately defining key particle characteristics required to achieve penetration of this barrier has proven critical to the design of efficacious drug-loaded particle systems (*30*, *31*). The ability to achieve brain penetration with larger particles (>100 nm) will enable higher drug-loading efficiency and payload, greater dispersion of drugs, and drug release over longer periods of time (*17*, *32*). These factors are known to correlate with the efficacy of many therapeutics (*11*, *17*) and will likely have a substantial impact on the use of nanosized carriers for diagnostic and therapeutic delivery to the brain. A recent study reported the construction of 100-nm gelatin particles that degraded into 10-nm particles when exposed to proteases within sarcoma tumors, with the goal of achieving better distribution with the smaller particle (*33*). Although an important goal for imaging agents, the very small particle size necessary to achieve penetration makes translation of a therapeutically effective controlled drug delivery system to humans less likely. Our results suggest that this system could be redesigned to degrade into particles as large as 114 nm, which may enhance drug and imaging agent options and improve the prospects for translation to the clinic. The demonstration here of the penetration within the brain by 85-nm PLGA-PEG NPs loaded with a chemotherapeutic (paclitaxel) bodes well for testing of this strategy in human clinical trials, either as a particle administered systemically that might reach brain tumors by the EPR effect or as a particle administered directly into the brain by CED.

Table 2. Effect of PEG coating density on NP penetration in rat brain tissue ex vivo. PEG surface density was calculated by NMR. Qualitative assessments of PS NP movement, scaled as (—) representing immobile NPs and (+++) representing highly diffusive NPs, were obtained by real-time MPT of NPs in rat brain tissue ex vivo (n = 4 videos per each of three brain samples).

Mean particle diameter ± SEM (nm)	Mean ζ potential ± SEM (mV)	PDI	PEG density (chains/100 nm^2)	Γ/SA	Qualitative MPT
119 ± 4	−9.8 ± 1.1	0.05	3	0.6	—
106 ± 3	−9.0 ± 0.8	0.03	3	0.7	—
111 ± 6	−8.5 ± 0.1	0.03	6	1.2	—
111 ± 3	−6.9 ± 0.5	0.04	7	1.7	–
119 ± 1	−5.5 ± 0.4	0.02	9	2.1	++
106 ± 4	−4.4 ± 0.2	0.03	9	2.0	+++
114 ± 3	−2.5 ± 0.1	0.03	9	2.0	+++

NPs have been shown to accumulate in the brain parenchyma after systemic administration in various disease models that have a disrupted BBB (*6*, *7*, *34*). Studies have further shown that PEG-coated polymer NPs accumulate much more efficiently in the parenchyma than do uncoated, but otherwise similar, NPs (*8*, *9*). In these papers, the PEG-coated particles were 135 to 165 nm in diameter and had a surface charge between −20 and −40 mV, suggesting that they may be too large and/or coated with an insufficiently dense layer of PEG to spread within the brain parenchyma after their uptake by the EPR effect. NPs coated with special surfactants, such as Polysorbate 80 (P80) (*5*, *34*) or Poloxamer 188 (also referred to as Pluronic F68) (*5*, *35*), or with chitosan (*36*) have also been shown to target the brain after systemic injection, even with an intact BBB, by adhering to and entering endothelial cells of the BBB. The NPs coated with P80 or F68 had surface charges in the −20 to −40 mV range, and the chitosan-coated particles were 260 nm in diameter, thereby making it unlikely that these specific particles are capable of spreading into the brain beyond the BBB endothelium. These previous papers, combined with our current findings, suggest that densely PEG-coated NPs with sizes ≤114 nm and a near-neutral surface charge may allow both accumulation within the brain after systemic administration and efficient spread by diffusion within the brain parenchyma in diseases with an impaired BBB.

Early measurements of the ECS pore size with electron microscopy suggested the upper pore size limit was about 20 nm (*37*). In 2006, Thorne and Nicholson analyzed the diffusion limitations of macromolecules (dextrans) and 35-nm PEG-coated NPs in the rat brain using in vivo epifluorescence microscopy (*16*). From these data, the apparent diffusion coefficients were calculated, and, using a fluid-filled pore model, they suggested that the rat cortical ECS has pores as large as 38 to 64 nm (*16*). We characterized a batch of these commercially available PEG-coated QDs (35 nm, −5.1 mV) and found that they did not diffuse rapidly within the rat brain tissue ex vivo. We then further coated these same particles with PEG (34 nm, −3.1 mV) and found that these could penetrate more rapidly. Thus, the precise batch of the commercially available QDs used by Thorne and Nicholson may have had a PEG coating that was too sparse to allow for rapid penetration in the brain parenchyma, and any adhesive interactions between the QDs and the ECS would result in an underestimation of brain ECS pore size.

A net negative surface charge should reduce NP electrostatic interactions within the brain owing to repulsion from negatively charged cell surfaces and extracellular matrix components (*14*, *38*). Here, we show that negatively charged (COOH-coated) particles with exposed hydrophobic PS regions exhibit hindered diffusion regardless of particle size. Often underappreciated, the hydrophobic interactions between particle surfaces and ECS components can be a source of adhesion (*39*). Adequate surface shielding (via PEG, for example) from these interactions is apparently crucial for diffusion of large particles in the brain. The formation of PEG coatings well into the brush regime likely limits exposure of hydrophobic NP surfaces that facilitate adhesion to the brain ECS. We report diffusive NP behavior for PEG conformations on 100-nm PS particles, with Γ/SA ≥2.0, whereas Γ/SA ≤1.7 was insufficient. The impact of PEG on biodegradable polymeric NPs and liposome size and surface charge has been shown to be dependent on PEG molecular weight, particle core, and PEG weight percent (*30*, *40*, *41*). The precise PEG coating densities required should be further confirmed with additional methods, such as matrix-assisted laser desorption/ionization–time-of-flight and atomic force microscopy, and will likely depend on the material being coated.

Here, we established that NPs at least as large as 114 nm, but smaller than 200 nm, can penetrate brain ECS if coated with a high density of 5-kD PEG. Large brain-penetrating NPs offer a greater degree of flexibility in designing delivery systems to produce a desired effect within the human brain. Dense PEG coatings are also known to be important for enhanced NP circulation within the bloodstream and entering the brain through a disrupted BBB, and are also expected to lead to greater drug distribution when used with local strategies such as CED. Although we did not test in a disease model to confirm, demonstration of an 85-nm drug-loaded biodegradable NP that penetrates within the brain parenchyma suggests that the development of drug delivery systems with the characteristics established in this paper offers promising new directions for particle-mediated delivery of therapeutic molecules in the brain. We envision that our findings may be first translated into the clinic in the treatment of malignant brain tumors owing to the poor prognosis with this disease, where NPs may access the brain via the EPR effect and then spread locally to provide a more uniform delivery of encapsulated therapeutic agents. Alternatively, the NPs may be administered locally by CED to maximize their penetration to treat invasive tumor cells. Once safety has been established, this approach may find use in treating other CNS diseases or conditions associated with a disrupted BBB. In the future, we expect new methods that enhance the delivery of NPs into the brain through an intact BBB will be developed and shown to be safe, such as high-intensity focused ultrasound (*42*), thus leading to widespread clinical use of PEG-coated NPs.

MATERIALS AND METHODS

NP preparation and characterization

Red fluorescent COOH-modified PS particles (40 to 200 nm) (Molecular Probes) were covalently modified with methoxy (MeO)–PEG–amine (NH_2) (molecular size, 5 kD; Creative PEGWorks) by COOH-amine reaction, following a modified protocol described previously (*18*, *43*). These two protocols were combined and optimized here to obtain dense PEG coatings, a near-neutral ζ potential, and low PDI for 40- to 200-nm PS particles. Briefly, 100 μl of PS particle suspension was washed and resuspended to fourfold dilution in ultrapure water. An excess of MeO-PEG-NH_2 was added to the particle suspension and mixed to dissolve the PEG. *N*-Hydroxysulfosuccinimide (Sigma) was added to a final concentration of 7 mM, and 200 mM borate buffer (pH 8.2) was added to a fourfold dilution of the starting volume. 1-Ethyl-3-(3-dimethylaminopropyl) carbodiimide (EDC, Invitrogen) was added to a concentration of 10 mM. Particle suspensions were placed on a rotary incubator for 4 hours at 25°C and then centrifuged (Amicon Ultra-0.5 mL 100 K MWCO; Millipore). Particles were resuspended in ultrapure water to the initial particle volume (100 μl) and stored at 4°C until use.

The net surface charge (ζ potential), PDI, and hydrodynamic diameter were measured for COOH- and PEG-coated fluorescent NPs of all sizes. Particle characterization is described in detail in the Supplementary Methods.

Human and rat neocortical slice preparation

Human tissue collection was approved by the Institutional Review Board at Johns Hopkins University. Fresh human brain cortex was removed from five patients undergoing surgery for mesial temporal lobe epilepsy. After removal, the tissue was rapidly divided into the components needed for pathological analysis; the remaining tissue

was dissected to avoid the sclerotic tissue that often accompanies the disease and then placed in normal saline on ice and transported immediately to the laboratory for slice preparation. The tissue was immersed in chilled ACSF (Harvard Apparatus) supplemented with 10 mM glucose. Coronal slices (n = 6 per patient) were prepared with a rodent brain slice matrix kit (Zivic Instruments). The matrix and razor blades were washed with 0.9% normal saline and placed on ice before inserting the excised human brain sample. Sectioning of the brain was carried out on the basis of instrument instructions such that 1-mm-thick slices were obtained. Slices were placed in a petri dish containing ACSF. Individual slices were then placed in an eight-well glass chamber (Lab-Tek), and 200 μl of ACSF was added to each well, with no liquid at the tissue-well interface to minimize interference with movie capture. A 0.5-μl PS bead suspension was added to the gray matter region. The eight-well chamber was then incubated at 37°C in humidity chamber for 30 min before imaging to allow tissue recovery and convection dissipation (*44*).

For rat brain tissue slices, all experiments were carried out at Johns Hopkins University School of Medicine in accordance with National Institutes of Health guidelines and local Institutional Animal Care and Use Committee regulations. Brain tissue slices were prepared from 130- to 160-g female Sprague-Dawley rats. Animals were anesthetized with ketamine-xylazine and then administered an intracardiac injection of Euthasol. After euthanasia, the brain was rapidly removed and immersed in chilled ACSF supplemented with 10% glucose. Slices were processed, and biodegradable particles were added in the same way as the human cortical slice preparation and PS particle addition above. MPT analysis is described in the Supplementary Methods.

Histopathological analysis of human brain slices

The human brain tissue slices were studied with standard H&E staining to identify any changes in histological architecture and cell morphology introduced by the preparation and incubation process. Representative tissue slices (n = 4) were preserved in formalin immediately after sectioning in the laboratory and after completing data acquisition, about 3 hours after removal, preparation, incubation, and particle imaging. The tissue was removed from the formalin after 24 hours and placed in 70% ethanol solution until paraffin embedding, sectioning, and H&E staining. The tissue sections were examined by a board-certified neuropathologist (C.E.) for evidence of tissue changes or damage.

In vivo mouse brain imaging

All experiments were approved by the Institutional Animal Care and Use Committee. The in vivo mouse model used was optimized to minimize tissue injury and brain movement with respect to imaging, and experiments were designed with knowledge of the potential contributions to particle movement by regional micropulsations from the dense network of surrounding blood vessels, as well as bulk flow phenomenon known to contribute to interstitial fluid circulation within the brain (*45*, *46*). The cranial window technique was based on a modification from previously published studies (*47*, *48*). To create a stable, immobile cranial window, we placed a warm agarose solution (20%, w/v) over the exposed brain region, and a 5-mm glass coverslip was quickly placed before agarose cooling and gelatinization. A custom circular metal bar was secured to the adjacent bone just lateral to the sagittal suture with a small drop of fast-drying adhesive. Cement (HyBond Inc.) was then applied to secure the agarose, glass, and metal bar construct rigidly to the calvarium. A channel representing about 90° of the cover glass circle was not cemented and left exposed for the glass pipette to insert into the brain.

The cranial bar was secured to a custom microscope stage, allowing stable imaging of the anesthetized mouse. An upright confocal microscope (Zeiss Inc.) with a two-photon laser source (Coherent Inc.) tuned to 910 nm was used for imaging through a 20× microscope objective [Zeiss Inc., Plan-Apochromat (numerical aperture, 1.0; working distance, 1.9 mm)]. Images were collected with a non-descanned detector. The micro-injection apparatus attached to a stereotactic manipulator (Drummond Scientific Inc.) was fixed with a glass micropipette (tip diameter, ~30 μm), loaded with NP solution, and positioned for injection through the agarose channel into the brain. A blood vessel–free region of cortex was identified, and the micropipette was inserted to a depth of 100 to 200 μm below the pial surface under direct visualization, and withdrawn slightly to create a small pocket to receive the injection. The nano-injection device was set to inject 9.2 nl of particle solution at a rate of 23 nl/s. Particle combinations were mixed and injected at equivalent concentrations to each other, and data were captured every 5 min for 60 min.

Statistical analysis

Statistical analysis of data was performed by one-way ANOVA followed by Tukey honestly significant difference or Games-Howell tests with SPSS 18.0 software (IBM Inc.). Differences were considered statistically significant at $P < 0.05$.

SUPPLEMENTARY MATERIALS

www.sciencetranslationalmedicine.org/cgi/content/full/4/149/149ra119/DC1
Methods
Movie S1. Multiple particle tracking of 91-nm PLGA NPs in normal rat brain tissue ex vivo.
Movie S2. Multiple particle tracking of 83-nm paclitaxel-loaded PEG-PLGA NPs in normal rat brain tissue ex vivo.

REFERENCES AND NOTES

1. S. Wohlfart, S. Gelperina, J. Kreuter, Transport of drugs across the blood–brain barrier by nanoparticles. *J. Control. Release* **161**, 264–273 (2012).
2. L. P. Serwer, C. D. James, Challenges in drug delivery to tumors of the central nervous system: An overview of pharmacological and surgical considerations. *Adv. Drug Deliv. Rev.* **64**, 590–597 (2012).
3. C. Roney, P. Kulkarni, V. Arora, P. Antich, F. Bonte, A. Wu, N. N. Mallikarjuana, S. Manohar, H. F. Liang, A. R. Kulkarni, H. W. Sung, M. Sairam, T. M. Aminabhavi, Targeted nanoparticles for drug delivery through the blood–brain barrier for Alzheimer's disease. *J. Control. Release* **108**, 193–214 (2005).
4. Y. Matsumura, H. Maeda, A new concept for macromolecular therapeutics in cancer chemotherapy: Mechanism of tumoritropic accumulation of proteins and the antitumor agent smancs. *Cancer Res.* **46**, 6387–6392 (1986).
5. A. Ambruosi, S. Gelperina, A. Khalansky, S. Tanski, A. Theisen, J. Kreuter, Influence of surfactants, polymer and doxorubicin loading on the anti-tumour effect of poly(butyl cyanoacrylate) nanoparticles in a rat glioma model. *J. Microencapsul.* **23**, 582–592 (2006).
6. S. Kannan, H. Dai, R. S. Navath, B. Balakrishnan, A. Jyoti, J. Janisse, R. Romero, R. M. Kannan, Dendrimer-based postnatal therapy for neuroinflammation and cerebral palsy in a rabbit model. *Sci. Transl. Med.* **4**, 130ra46 (2012).
7. M. K. Reddy, V. Labhasetwar, Nanoparticle-mediated delivery of superoxide dismutase to the brain: An effective strategy to reduce ischemia-reperfusion injury. *FASEB J.* **23**, 1384–1395 (2009).
8. I. Brigger, J. Morizet, G. Aubert, H. Chacun, M. J. Terrier-Lacombe, P. Couvreur, G. Vassal, Poly(ethylene glycol)-coated hexadecylcyanoacrylate nanospheres display a combined effect for brain tumor targeting. *J. Pharmacol. Exp. Ther.* **303**, 928–936 (2002).
9. P. Calvo, B. Gouritin, H. Chacun, D. Desmaële, J. D'Angelo, J. P. Noel, D. Georgin, E. Fattal, J. P. Andreux, P. Couvreur, Long-circulating PEGylated polycyanoacrylate nanoparticles as new drug carrier for brain delivery. *Pharm. Res.* **18**, 1157–1166 (2001).
10. R. Gref, Y. Minamitake, M. T. Peracchia, V. Trubetskoy, V. Torchilin, R. Langer, Biodegradable long-circulating polymeric nanospheres. *Science* **263**, 1600–1603 (1994).

11. T. Patel, J. Zhou, J. M. Piepmeier, W. M. Saltzman, Polymeric nanoparticles for drug delivery to the central nervous system. *Adv. Drug Deliv. Rev.* **64**, 701–705 (2012).
12. J. W. Degen, S. Walbridge, A. O. Vortmeyer, E. H. Oldfield, R. R. Lonser, Safety and efficacy of convection-enhanced delivery of gemcitabine or carboplatin in a malignant glioma model in rats. *J. Neurosurg.* **99**, 893–898 (2003).
13. R. H. Bobo, D. W. Laske, A. Akbasak, P. F. Morrison, R. L. Dedrick, E. H. Oldfield, Convection-enhanced delivery of macromolecules in the brain. *Proc. Natl. Acad. Sci. U.S.A.* **91**, 2076–2080 (1994).
14. E. Allard, C. Passirani, J. P. Benoit, Convection-enhanced delivery of nanocarriers for the treatment of brain tumors. *Biomaterials* **30**, 2302–2318 (2009).
15. A. Pluen, Y. Boucher, S. Ramanujan, T. D. McKee, T. Gohongi, E. di Tomaso, E. B. Brown, Y. Izumi, R. B. Campbell, D. A. Berk, R. K. Jain, Role of tumor–host interactions in interstitial diffusion of macromolecules: Cranial vs. subcutaneous tumors. *Proc. Natl. Acad. Sci. U.S.A.* **98**, 4628–4633 (2001).
16. R. G. Thorne, C. Nicholson, In vivo diffusion analysis with quantum dots and dextrans predicts the width of brain extracellular space. *Proc. Natl. Acad. Sci. U.S.A.* **103**, 5567–5572 (2006).
17. R. Langer, Drug delivery and targeting. *Nature* **392**, 5–10 (1998).
18. S. K. Lai, D. E. O'Hanlon, S. Harrold, S. T. Man, Y. Y. Wang, R. Cone, J. Hanes, Rapid transport of large polymeric nanoparticles in fresh undiluted human mucus. *Proc. Natl. Acad. Sci. U.S.A.* **104**, 1482–1487 (2007).
19. Y. Y. Wang, S. K. Lai, J. S. Suk, A. Pace, R. Cone, J. Hanes, Addressing the PEG mucoadhesivity paradox to engineer nanoparticles that "slip" through the human mucus barrier. *Angew. Chem. Int. Ed. Engl.* **47**, 9726–9729 (2008).
20. B. Amsden, An obstruction-scaling model for diffusion in homogeneous hydrogels. *Macromolecules* **32**, 874–879 (1999).
21. S. K. Lai, Y. Y. Wang, K. Hida, R. Cone, J. Hanes, Nanoparticles reveal that human cervicovaginal mucus is riddled with pores larger than viruses. *Proc. Natl. Acad. Sci. U.S.A.* **107**, 598–603 (2010).
22. A. Peters, Golgi, Cajal, and the fine structure of the nervous system. *Brain Res. Rev.* **55**, 256–263 (2007).
23. A. van Harreveld, Extracellular space in the central nervous system. *Proc. K. Ned. Akad. Wet. C* **69**, 17–21 (1966).
24. M. E. Rice, C. Nicholson, Diffusion characteristics and extracellular volume fraction during normoxia and hypoxia in slices of rat neostriatum. *J. Neurophysiol.* **65**, 264–272 (1991).
25. Y. Ibata, F. Piccoli, G. D. Pappas, A. Lajtha, An electron microscopic and biochemical study on the effect of cyanide and low Na^+ on rat brain slices. *Brain Res.* **30**, 137–158 (1971).
26. S. de Boüard, C. Christov, J. S. Guillamo, L. Kassar-Duchossoy, S. Palfi, C. Leguerinel, M. Masset, O. Cohen-Hagenauer, M. Peschanski, T. Lefrançois, Invasion of human glioma biopsy specimens in cultures of rodent brain slices: A quantitative analysis. *J. Neurosurg.* **97**, 169–176 (2002).
27. K. L. Chaichana, V. Capilla-Gonzalez, O. Gonzalez-Perez, G. Pradilla, J. Han, A. Olivi, H. Brem, J. M. Garcia-Verdugo, A. Quiñones-Hinojosa, Preservation of glial cytoarchitecture from ex vivo human tumor and non-tumor cerebral cortical explants: A human model to study neurological diseases. *J. Neurosci. Methods* **164**, 261–270 (2007).
28. F. Hajós, B. Gerics, P. Sótonyi, Slices from the rat olfactory bulb maintained in vitro. Morphological aspects. *J. Neurosci. Methods* **44**, 225–232 (1992).
29. A. U. Larkman, A. Mason, C. Blakemore, The in vitro slice preparation for combined morphological and electrophysiological studies of rat visual cortex. *Neurosci. Res.* **6**, 1–19 (1988).
30. B. C. Tang, M. Dawson, S. K. Lai, Y. Y. Wang, J. S. Suk, M. Yang, P. Zeitlin, M. P. Boyle, J. Fu, J. Hanes, Biodegradable polymer nanoparticles that rapidly penetrate the human mucus barrier. *Proc. Natl. Acad. Sci. U.S.A.* **106**, 19268–19273 (2009).
31. L. M. Ensign, B. C. Tang, Y. Y. Wang, T. A. Tse, T. Hoen, R. Cone, J. Hanes, Mucus-penetrating nanoparticles for vaginal drug delivery protect against herpes simplex virus. *Sci. Transl. Med.* **4**, 138ra79 (2012).
32. D. H. Kim, D. C. Martin, Sustained release of dexamethasone from hydrophilic matrices using PLGA nanoparticles for neural drug delivery. *Biomaterials* **27**, 3031–3037 (2006).
33. C. Wong, T. Stylianopoulos, J. Cui, J. Martin, V. P. Chauhan, W. Jiang, Z. Popovic, R. K. Jain, M. G. Bawendi, D. Fukumura, Multistage nanoparticle delivery system for deep penetration into tumor tissue. *Proc. Natl. Acad. Sci. U.S.A.* **108**, 2426–2431 (2011).
34. A. Ambruosi, A. S. Khalansky, H. Yamamoto, S. E. Gelperina, D. J. Begley, J. Kreuter, Biodistribution of polysorbate 80-coated doxorubicin-loaded [^{14}C]-poly(butyl cyanoacrylate) nanoparticles after intravenous administration to glioblastoma-bearing rats. *J. Drug Target.* **14**, 97–105 (2006).
35. S. A. Kulkarni, S. S. Feng, Effects of surface modification on delivery efficiency of biodegradable nanoparticles across the blood–brain barrier. *Nanomedicine* **6**, 377–394 (2011).
36. J. H. Na, H. Koo, S. Lee, K. H. Min, K. Park, H. Yoo, S. H. Lee, J. H. Park, I. C. Kwon, S. Y. Jeong, K. Kim, Real-time and non-invasive optical imaging of tumor-targeting glycol chitosan nanoparticles in various tumor models. *Biomaterials* **32**, 5252–5261 (2011).
37. B. Cragg, Preservation of extracellular space during fixation of the brain for electron microscopy. *Tissue Cell* **12**, 63–72 (1980).
38. E. Syková, C. Nicholson, Diffusion in brain extracellular space. *Physiol. Rev.* **88**, 1277–1340 (2008).
39. V. Vyas, A. Podestà, P. Milani, Probing nanoscale interactions on biocompatible cluster-assembled titanium oxide surfaces by atomic force microscopy. *J. Nanosci. Nanotechnol.* **11**, 4739–4748 (2011).
40. S. Pamujula, S. Hazari, G. Bolden, R. A. Graves, D. D. Chinta, S. Dash, V. Kishore, T. K. Mandal, Cellular delivery of PEGylated PLGA nanoparticles. *J. Pharm. Pharmacol.* **64**, 61–67 (2012).
41. O. Mert, S. K. Lai, L. Ensign, M. Yang, Y. Y. Wang, J. Wood, J. Hanes, A poly(ethylene glycol)-based surfactant for formulation of drug-loaded mucus penetrating particles. *J. Control. Release* **157**, 455–460 (2012).
42. N. McDannold, C. D. Arvanitis, N. Vykhodtseva, M. S. Livingstone, Temporary disruption of the blood–brain barrier by use of ultrasound and microbubbles: Safety and efficacy evaluation in rhesus macaques. *Cancer Res.* **72**, 3652–3663 (2012).
43. S. R. Popielarski, S. H. Pun, M. E. Davis, A nanoparticle-based model delivery system to guide the rational design of gene delivery to the liver. 1. Synthesis and characterization. *Bioconjug. Chem.* **16**, 1063–1070 (2005).
44. K. Rambani, J. Vukasinovic, A. Glezer, S. M. Potter, Culturing thick brain slices: An interstitial 3D microperfusion system for enhanced viability. *J. Neurosci. Methods* **180**, 243–254 (2009).
45. N. J. Abbott, Evidence for bulk flow of brain interstitial fluid: Significance for physiology and pathology. *Neurochem. Int.* **45**, 545–552 (2004).
46. O. Sato, E. A. Bering Jr., M. Yagi, R. Tsugane, M. Hara, Y. Amano, T. Asai, Bulk flow in the cerebrospinal fluid system of the dog. *Acta Neurol. Scand.* **51**, 1–11 (1975).
47. D. D. Bock, W. C. Lee, A. M. Kerlin, M. L. Andermann, G. Hood, A. W. Wetzel, S. Yurgenson, E. R. Soucy, H. S. Kim, R. C. Reid, Network anatomy and in vivo physiology of visual cortical neurons. *Nature* **471**, 177–182 (2011).
48. A. Holtmaat, T. Bonhoeffer, D. K. Chow, J. Chuckowree, V. De Paola, S. B. Hofer, M. Hübener, T. Keck, G. Knott, W. C. Lee, R. Mostany, T. D. Mrsic-Flogel, E. Nedivi, C. Portera-Cailliau, K. Svoboda, J. T. Trachtenberg, L. Wilbrecht, Long-term, high-resolution imaging in the mouse neocortex through a chronic cranial window. *Nat. Protoc.* **4**, 1128–1144 (2009).
49. V. Rizzo, V. Pinciroli, Quantitative NMR in synthetic and combinatorial chemistry. *J. Pharm. Biomed. Anal.* **38**, 851–857 (2005).
50. H. S. Yoo, J. E. Oh, K. H. Lee, T. G. Park, Biodegradable nanoparticles containing doxorubicin-PLGA conjugate for sustained release. *Pharm. Res.* **16**, 1114–1118 (1999).
51. M. T. Valentine, Z. E. Perlman, M. L. Gardel, J. H. Shin, P. Matsudaira, T. J. Mitchison, D. A. Weitz, Colloid surface chemistry critically affects multiple particle tracking measurements of biomaterials. *Biophys. J.* **86**, 4004–4014 (2004).

Acknowledgments: We thank F. Lenz, G. Jallo, A. Quinones-Hinojosa, W. Hsu, and J. Liauw for the help in providing human tissue samples. We thank H. Brem and B. Tyler for their advice and guidance on clinical applications and animal surgery techniques, respectively. **Funding:** This work was supported by NIH grants R01CA164789, 5T32CA130840-02, and U54CA151838. **Author contributions:** G.F.W., E.A.N., and J.H. developed the concept. E.A.N. and G.F.W. designed and performed ex vivo experiments. G.F.W. established arrangements for human tissue. G.F.W., E.A.N., and K.A.S. designed and performed in vivo experiments. E.A.N. and T.-Y.S. designed and performed biodegradable particle experiments. Q.X. performed NMR experiments and analysis. E.A.N., G.F.W., T.-Y.S., G.S., and D.X. analyzed the data. C.E. provided histological analysis for all tissues. E.A.N., G.F.W., and J.H. wrote the paper. **Competing interests:** The content is solely the responsibility of the authors and does not necessarily represent the official views of the NIH. E.A.N., G.F.W., and J.H. are inventors on a pending patent (WO 2012/039979) related to this work.

Submitted 12 December 2011
Accepted 10 July 2012
Published 29 August 2012
10.1126/scitranslmed.3003594

Citation: E. A. Nance, G. F. Woodworth, K. A. Sailor, T.-Y. Shih, Q. Xu, G. Swaminathan, D. Xiang, C. Eberhart, J. Hanes, A dense poly(ethylene glycol) coating improves penetration of large polymeric nanoparticles within brain tissue. *Sci. Transl. Med.* **4**, 149ra119 (2012).

Science Translational Medicine

A Dense Poly(Ethylene Glycol) Coating Improves Penetration of Large Polymeric Nanoparticles Within Brain Tissue

Elizabeth A. Nance, Graeme F. Woodworth, Kurt A. Sailor, Ting-Yu Shih, Qingguo Xu, Ganesh Swaminathan, Dennis Xiang, Charles Eberhart and Justin Hanes

Sci Transl Med **4**, 149ra119149ra119.
DOI: 10.1126/scitranslmed.3003594

Brain-Penetrating Particles

It was once thought that particles larger than 60 nm would be stuck in the brain extracellular space (ECS), unable to penetrate further. This has been a particularly bothersome rule of thumb for the design of drug delivery systems that rely on larger particles or viruses to carry therapeutics. Now, Nance and colleagues have challenged this hypothesis by exploring particles that are >60 nm, discovering that large particles, with the right coating, can indeed diffuse throughout the ECS of both rat and human brains.

The authors first coated fluorescent polystyrene particles with a dense layer of the bio-inert polymer poly(ethylene glycol) (commonly known as PEG) or with a carboxyl moiety (COOH). Using a multiple-particle tracking method, the authors reported that 114-nm PEG-coated particles penetrated ex vivo human brain tissue with ease, whereas similarly sized COOH-coated particles were stopped in their tracks. Nance *et al.* attributed this difference to the dense, near-neutral PEG coating, claiming that it allows the particles to experience the brain ECS more as a fluid than an impermeable solid. The importance of the PEG coating was further confirmed in living mice, where real-time video microscopy revealed that the 100-nm PEG-coated particles penetrated farther into the mouse brain than the 100-nm COOH-coated ones.

With a brain ECS pore size cutoff >100 nm, many doors can be opened in nanomedicine. Larger particles permit the inclusion of higher quantities of drug, which can be distributed for longer periods of time to more areas within the brain. Nance and colleagues preliminarily demonstrated such drug delivery capabilities using paclitaxel-loaded, 85-nm biodegradable nanoparticles, showing that only particles with the PEG coating could diffuse rapidly throughout rat brain tissue ex vivo. Although these densely coated particles may make drug delivery more efficient, they have yet to be tested in a disease model to confirm efficacy over conventional nanoparticles. Although currently limited to direct infusion into the brain, for eventual use in humans, it is hoped that they may be administered systemically for treating diseases with an impaired blood-brain barrier.